On the Performance of TCP over Free-Space Optical Atmospheric Turbulence Channels

Vuong V. Mai, Truong C. Thang, and Anh T. Pham

***Abstract*—This paper presents an analytical study on the performance of transmission control protocol (TCP) over free-space optical (FSO) turbulence channel when the automatic-repeat request, selective repeat (ARQ-SR) scheme is used by the link layer. Different TCP versions, including Tahoe, Reno and selective acknowledgement (SACK), are considered. In the analysis of TCP throughput, a three-dimensional (3-D) Markov model is used. In addition, to analyze the joint effect of ARQ-SR and FSO turbulence channel in terms of both TCP throughput and the energy consumption, a newly defined energy-throughput efficiency parameter is analytically derived. In the numerical results, we discuss cross-layer designing strategies for the selection of FSO system parameters and ARQ-SR scheme in order to maximize the TCP throughput, and to achieve the trade-off between the energy consumption and the throughput in various conditions of the FSO turbulence channel.**

***Index Terms*—FSO Communications; Atmospheric Turbulence; TCP; ARQ-SR.**

I. Introduction

Free-space optical (FSO) communications is a transmission technology in which the optical signal is transmitted through the atmosphere. FSO has been considered as an alternative solution for a wide range of applications thanks to its advantages such as license-free, high data rate, quick and easy deployment, and cost-effectiveness [1]. In FSO systems, one of major issues is the high error rate due to the impact of the atmospheric turbulence [2]. Over the past decade or so, there have been many studies focusing on the effect of atmospheric turbulence on the performance of physical layer in FSO systems [3]–[7].

In the transport layer, to offer a reliable transmission, the popular Transmission Control Protocol (TCP) is employed to carried many internet applications, including FTP, TELNET, E-mail, etc. However, it has been proven that the TCP performance is severely degraded when it is operating over high error-rate environments, including both radio and optical wireless (e.g. FSO) communications [10]–[13]. Therefore, such environments pose formidable challenges to maintain the TCP reliability.

In radio wireless communications, many proposals to overcome the degradation of TCP performance have been reported [8]–[12]. These proposals can be categorized into two groups. The first one includes methods to modify the TCP congestion operation to adapt to the multiple segment loss in wireless transmission [8]. In another group, the TCP performance is enhanced by employing new schemes in the link layer. For example, in [9], the explicit loss notification (ELN) scheme has been proposed to provide TCP with the ability to classify wireless link losses and congestion losses. The TCP-sender therefore can react appropriately with each case of losses. In addition, error recovery schemes in the link layer, such as the automatic-repeat request (ARQ)-based retransmission of the error data [10]–[11] and the forward error correction (FEC) [12], have also been introduced. It is seen in these studies that, the interaction between the designs of link layer and wireless physical layer plays an importance role to improve the TCP performance at the transport layer.

Regarding the FSO communications, there have been recently several studies focusing on the performance of transport and link layers over the FSO turbulence channels [13]–[16]. In [13], Lee *et al.* focused solely on the transport layer and analyzed the TCP throughput over the clear atmospheric turbulence channels. It is seen that the TCP throughput strongly depends upon the atmospheric turbulence and the channel distance. In [14]–[16], the outage probability of FSO systems when the ARQ and FEC schemes are used in the link layer has been studied taking into account the FSO log-normal turbulence channels. In these studies, the impact of FSO channel conditions on the performance of either link or transport layer has been separately studied.

Similar to the radio wireless communications, the understanding of the combined impact of both link and physical layers on the performance of TCP would result in more efficient cross-layer optimization. This is especially critical to the design of the FSO networks due to the harsh condition of atmospheric channels. In this paper, we therefore develop an analytical framework for cross-layer performance analysis of transport layer performance considering the effects from both FSO channel and link layer design. In our study, different TCP versions are considered and a three-dimensional (3-D) Markov chain model that includes the exponential back-off phase is used for modeling the TCP operation. It is important to include the exponential back-off phase as the probability of this event is considerably high in FSO link due to the burst loss caused by the atmospheric turbulence. In the link layer, we also employ the automatic-repeat request, selective repeat (ARQ-SR) scheme thanks to its ability to offer both loss-recovery efficiency and simplicity [14]–[16]. In the physical layer, the sub-carrier binary phase-shift keying (SC-BPSK) system, as described in [7], is employed and both FSO log-normal and gamma-gamma turbulence channels are considered for the case of weak-to-moderate and strong turbulences, respectively. In addition, we define a new parameter, the joint throughput-energy efficiency, which is the the ratio between the TCP throughput and the average energy for transmitting an unit data of TCP. Using this parameter, we can optimize FSO system parameters for the trade-off between the energy consumption and the TCP throughput in various contexts of ARQ-SR and FSO turbulence channels.

The remainder of the paper is organized as follows. The system descriptions, including the network model, FSO channel model and ARQ-SR scheme, are detailed in Section II. In Section III, TCP segment-loss probability and end-to-

The authors are with the Computer Communications Lab., The University of Aizu, Aizuwakamatsu, Fukushima, Japan 965-8580 (e-mail: pham@u-aizu.ac.jp).

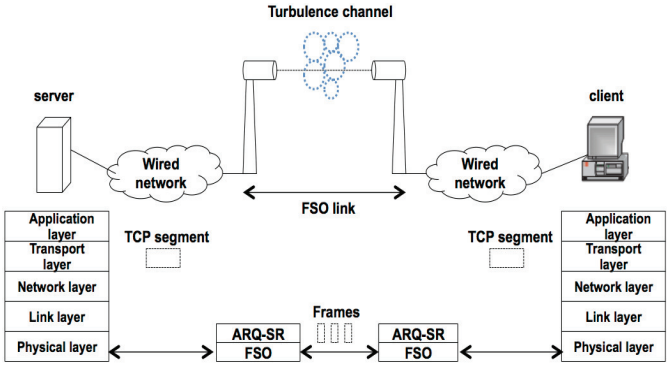

Fig. 1. Network scenario with a TCP connection over FSO link.

end transmission delay are derived considering the impact of link and physical layers. The TPC Markov chain model is presented in Section IV. The TCP performance analysis and numerical results are given in Section V and VI, respectively. Finally, Section VII concludes the paper.

II. System Descriptions

A. Network Model

Figure 1 illustrates the network scenario with an end-to-end TCP connection between a source (server) and a destination (client) over a FSO link and wired networks. At the physical layer of the FSO link the optical signal is transmitted over free space under the impact of atmospheric turbulence. We apply SC-BPSK as modulation scheme for the physical layer transmission. In addition, the log-normal and gamma-gamma models are assumed for the weak and strong atmospheric turbulence conditions, respectively.

In the data link layer each TCP segment of size L_{TCP} is divided into N_f smaller data units, i.e. frames, before transmitting over the FSO link. Under the impact of atmospheric turbulence, the frame error on FSO-link may happen frequently. Thus, the purpose of ARQ-SR is to retransmit the corrupted frames. In the transport layer, we employ one of TCP versions such as TCP-Reno, TCP-Tahoe and TCP-SACK; we assume that the reader is familiar with those TCP versions and thus neglect the description of TCP operation. Details of TCP operation can be found in [18].

B. FSO Channel Models

FSO channels, under the influence by the atmosphere-induced turbulence, can be modeled as fading channel. In case of weak turbulence, it is generally accepted that the influence of turbulence is modeled as a random process with log-normal distribution whose the probability density function (p.d.f) is given as

$$f_X(x) = \frac{1}{\sqrt{2\pi}\sigma_s x} \exp\left[-\frac{\left(\ln x + \sigma_s^2/2\right)^2}{2\sigma_s^2}\right], \quad (1)$$

where σ_s^2 is the log intensity variance that depends on the channel characteristics as given by [5]

$$\sigma_s^2 = \exp\left[\frac{0.49\sigma_R^2}{\left(1+0.18d^2+0.56\sigma_R^{12/5}\right)^{7/6}} + \frac{0.51\sigma_R^2}{\left(1+0.9d^2+0.62d^2\sigma_R^{12/5}\right)^{5/6}}\right] - 1. \quad (2)$$

Here, $d = \sqrt{kD^2/4L}$, $k = 2\pi/\lambda$ is the optical wave number, L is the channel distance, and D is the receiver aperture diameter. σ_R^2 is the Rytov variance, and in case of plane wave propagation, it is given by

$$\sigma_R^2 = 1.23 C_n^2 k^{7/6} L^{11/6}, \quad (3)$$

where C_n^2 is the altitude-dependent index of the refractive structure parameter determining the turbulence strength. Typically C_n^2 varies from 10^{-17} to 10^{-13} accordingly to the strength of atmospheric turbulence.

When the atmospheric turbulence becomes stronger (the strength is higher than 2×10^{-14}), it can be characterized by a stationary random process with gamma-gamma distribution whose p.d.f is described as

$$f_X(x) = \frac{2(\alpha\beta)^{(\alpha+\beta)/2}}{\Gamma(\alpha)\Gamma(\beta)} x^{(\alpha+\beta)/2-1} K_{\alpha-\beta}\left(2\sqrt{\alpha\beta x}\right), \quad (4)$$

where $\Gamma(.)$ is the gamma function, and $K_{\alpha-\beta}(.)$ is the modified Bessel function of the second kind and order $\alpha-\beta$. α and β are the p.d.f parameters describing the turbulence experienced by waves, and in the case of zero-inner scale they are given by [3]

$$\alpha = \left\{\exp\left[\frac{0.49\sigma_R^2}{\left(1+1.11\sigma_R^{12/5}\right)^{7/6}}\right] - 1\right\}^{-1},$$
$$\beta = \left\{\exp\left[\frac{0.51\sigma_R^2}{\left(1+0.69\sigma_R^{12/5}\right)^{5/6}}\right] - 1\right\}^{-1}. \quad (5)$$

Here, both σ_R^2 and d are also defined as in case of the log-normal channel mentioned above.

C. ARQ-SR Scheme

Basically, we can explain the operation of ARQ-SR as the activity of re-transmission of the corrupted frames. The maximum number of re-transmissions is determined by parameter M. If after M attempts of re-transmission, and the frame does not get through the FSO link, ARQ-SR gives up and the corresponding TCP segment is lost. In this Section, we analyze the performance of TCP taking into account the combined effect of the FSO link and ARQ-SR scheme. In particular, the TCP segment-loss probability and the average end-to-end transmission delay, which are two key TCP performance indicators, will be analytically derived.

III. TCP Segment Loss and Transmission Delay

A. TCP Segment-Loss Probability

Let P_{FSO} and P_{wire} denote the segment-loss probabilities in the FSO link and wired network, respectively, the probability of having exactly i losses out of w segments, $P_w(i)$, can

be expressed as

$$P_w(i) = \binom{w}{i} [1-(1-P_{FSO})(1-P_{wire})]^i \times [(1-P_{FSO})(1-P_{wire})]^{w-1}. \quad (6)$$

The TCP segment-loss probability on the FSO link under ARQ-SR scheme can be written as

$$P_{FSO} = 1 - \left(1 - P_f^{M+1}\right)^{N_f}, \quad (7)$$

in which P_f is the frame-error probability on the FSO link, and it can be given by

$$P_f = 1 - (1-P_e)^{L_f}, \quad (8)$$

where $L_f = [L_{TCP}/N_f]$ is the frame length and P_e is bit-error probability.

In FSO systems employing SC-BPSK, P_e is given as [7]

$$P_e = \int_0^\infty Q\left(\sqrt{\text{SNR}} \cdot x\right) f_X(x) dx, \quad (9)$$

where $Q(.)$ is the Gaussian Q-function with

$$Q(y) = \frac{1}{\sqrt{2\pi}} \int_y^\infty \exp(-\frac{y^2}{2}) dy, \quad (10)$$

and SNR is the signal-to-noise ratio, which can be expressed as

$$\text{SNR} = (\frac{m\Re P_s a}{4\sigma_N})^2, \quad (11)$$

where P_s is the peak transmitted power of the laser beam, m is the modulation index, $\Re$ is the responsivity of the photodetector at the receiver, σ_N^2 is the receiver noise variance and $a = D^2(\phi L)^{-2}\exp(-\beta L)$ is channel attenuation, in which D, L, ϕ and β are the receiver aperture diameter, the channel distance, the angle of divergence in radian, and the atmospheric extinction coefficient, respectively.

When the turbulence is modeled by log-normal channel, the system BER can be expressed as

$$P_e = \int_0^\infty Q\left(\sqrt{\text{SNR}} \cdot x\right) \times \times \frac{1}{\sqrt{2\pi}\sigma_s x} \exp\left[-\frac{(\ln x + \sigma_s^2/2)^2}{2\sigma_s^2}\right] dx. \quad (12)$$

Making the change of variable $y = \frac{(\ln x + \sigma_s^2/2)}{\sqrt{2}\sigma_s}$ we have

$$P_e = \frac{1}{\sqrt{\pi}} \int_{-\infty}^\infty Q\left[\sqrt{\text{SNR}} \cdot \exp(\sqrt{2}\sigma_s y - \sigma_s^2/2)\right] \times \times \exp(-y^2) dy. \quad (13)$$

Using the approximation

$$\int_{-\infty}^\infty g(y)\exp(-y^2)dy \approx \sum_{i=-N; i\neq 0}^N w_i g(y_i), \quad (14)$$

where w_i and y_i, in which $i = (-N, -N+1, ..., 1, 2, ..., N)$, are the weight factors and the zeros of the Hermite polynomial, respectively, we can obtain a tractable expression of P_e, that is

$$P_e \approx \frac{1}{\sqrt{\pi}} \sum_{i=-N; i\neq 0}^N w_i Q\left[\sqrt{\text{SNR}} \cdot \exp(\sqrt{2}\sigma_s y_i - \sigma_s^2/2)\right]. \quad (15)$$

For gamma-gamma channels the BER expression is given by

$$P_e = \int_0^\infty Q\left(\sqrt{\text{SNR}} \cdot x\right) \times \times \frac{2(\alpha\beta)^{(\alpha+\beta)/2}}{\Gamma(\alpha)\Gamma(\beta)} x^{(\alpha+\beta)/2-1} K_{\alpha-\beta}\left(2\sqrt{\alpha\beta x}\right) dx. \quad (16)$$

This integral can be solved by use of a series expansion for modified Bessel function [6], $K_v(y)$, with

$$K_v(y) = \frac{\pi}{2sin(\pi v))} \sum_{p=0}^\infty [\frac{(y/2)^{2p-v}}{\Gamma(p-v+1)p!} - \frac{(y/2)^{2p+v}}{\Gamma(p+v+1)p!}], v \notin \mathbb{Z}, |y| < \infty. \quad (17)$$

Based on the derivation in [4], we can substitute Eq. (17) into Eq. (16) in order to obtain the close form of P_e as follows:

$$P_e = A(\alpha,\beta) \sum_{p=0}^\infty [a_p(\alpha,\beta) B(\frac{1}{2}, \frac{p+\beta+1}{2}) (\frac{\text{SNR}}{2})^{-\frac{p+\beta}{2}} - - a_p(\beta,\alpha) B(\frac{1}{2}, \frac{p+\alpha+1}{2}) (\frac{\text{SNR}}{2})^{-\frac{p+\alpha}{2}}], \quad (18)$$

where $B(x,y) = \frac{\Gamma(x)\Gamma(y)}{\Gamma(x)+\Gamma(y)}$ is the Beta function. $A(\alpha,\beta)$ and $a_p(x,y)$ are given by

$$A(\alpha,\beta) = \frac{1}{4\Gamma(\alpha)\Gamma(\beta)\text{sin}[(\alpha-\beta)\pi]}, \quad (19)$$

$$a_p(x,y) = \frac{(xy)^{p+y}\Gamma(\frac{p+y}{2})}{\Gamma(p-x+y+1)p!}. \quad (20)$$

B. Average TCP End-to-End Transmission Delay

The average end-to-end transmission delay or the average round-trip time, $E[RTT]$, can be defined as the average of time period from the time when TCP source transmits a segment to the time when the corresponding ACK comes back to the source. It is derived as follows:

$$E[RTT] = 2 \times T_{wire} + (L_f/R + T_{CRC})(\overline{M}+1)N_f, \quad (21)$$

where T_{wire} is the one way transmission time in the wired part. R is the transmission rate of FSO link. T_{CRC} is the error detection time that data-link layer spends to check the CRC field and recognize the corrupted frame. L_f/R is the time needed for the transmission of one frame. $\overline{M}$ is the average number of re-transmissions for one frame, which depends on the operation ARQ-SR and the frame loss probability on FSO link and is determined as

$$\begin{aligned}\overline{M} &= \sum_{m=0}^M m\frac{P_f^m(1-P_f)}{1-P_f^{M+1}} = \frac{P_f(1-P_f)}{1-P_f^{M+1}} \sum_{m=1}^M mP_f^{m-1} \\ &= \frac{P_f(1-P_f)}{1-P_f^{M+1}} \frac{\partial}{\partial P_f}\left(\frac{1-P_f^{M+1}}{1-P_f}\right) \\ &= \frac{P_f(1-P_f)}{1-P_f^{M+1}} \frac{-(M+1)P_f^M(1-P_f)+(1-P_f^{M+1})}{(1-P_f)^2} \\ &= \frac{P_f}{1-P_f} - \frac{(M+1)P_f^{M+1}}{1-P_f^{M+1}}. \end{aligned} \quad (22)$$

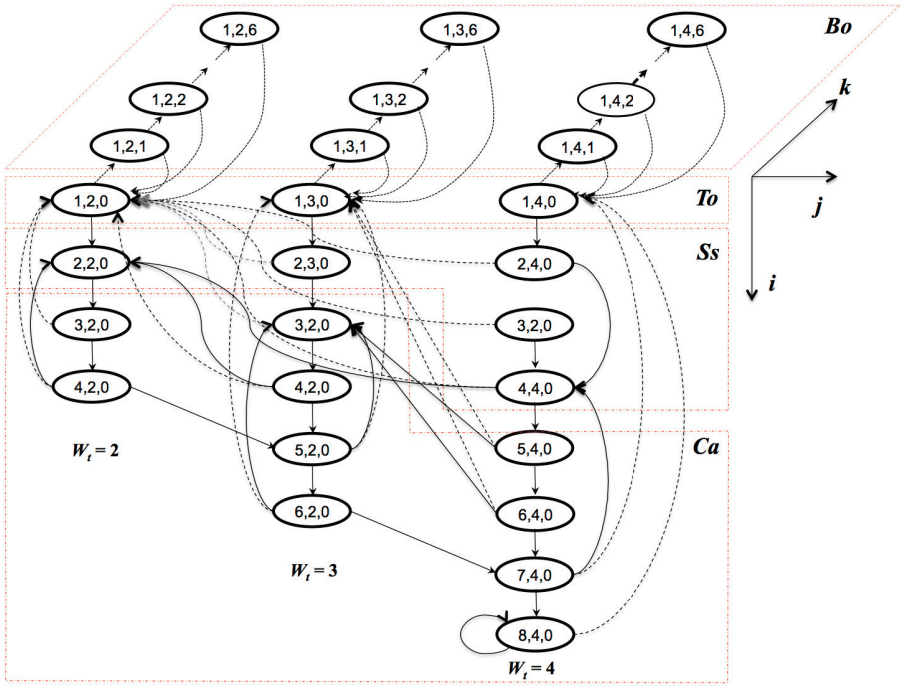

Fig. 2. Markov chain model for $W_{max} = 8$ and the number of increasing timeouts is limited by 6.

IV. TCP Operation Model

In this section, we present the 3-D Markov chain model, which includes the exponential back-off phase, to analytically study the performance of TCP over FSO link with ARQ-SR. It is necessary to note that the exponential back-off phase was omitted in [13]. In FSO link, it is necessary to include the exponential back-off phase in the TCP analysis. The reason is that the temporal correlation time of the atmospheric turbulence process is on the order of several milliseconds, burst error often occurs in the FSO link. In addition, in order to study the performance of different TCP versions, we first create the Markov chain model for TCP-Reno and then expand it for TCP-Tahoe and TCP-SACK.

A. 3-D Markov Chain Structure

The behavior of the TCP-Reno can be modeled as a 3-D Markov chain as shown in Fig. 2. In this figure, the three axes (i, j, k) represents the congestion window size, the value of slow-start threshold and the number of increasing timeouts in the exponential back-off phase, respectively. Here we assume that the maximum window size $W_{max} = 8$, the number of increasing timeouts is limited by 6. Furthermore, the timeout increasing factor of 2 is selected (i.e. we have the binary exponential back-off), and therefore the equivalent maximum timeout duration is 2^6T.

In the figure, the TCP-Reno operation can be separated into four sections according to the four operating phases: slow-start, congestion avoidance, timeout, and exponential back-off. Initially, the congestion window is set to one segment and in slow-start phase (Ss), if there is no loss event, the congestion window is doubled after each RTT. Its growth continues until it reaches the current slow-start threshold (W_t); then TCP-Reno changes into the congestion avoidance phase (Ca). In Ca, if there is no loss occurring, the window size will increase by one segment per RTT. This increase in window size continues until either the congestion window reaches the maximum window size (W_{max}), or there is a loss event.

If the loss event is a triple-duplicate ACK, TCP-Reno will reduce the congestion window size to a half, and continues staying in the Ca phase. If a timeout occurs, TCP-Reno will fall into time-out phase (To) and set the slow-start threshold to a half of the current congestion window size. TCP will wait for a timeout duration, T, before trying to transmit a segment. If this segment is lost again, TCP will double the timeout period. This doubling is known as the exponential back-off phase (Bo). Bo continues up to a maximum timeout value of 2^6T before exiting and coming back to To.

Finally, the general state space E of the Markov chain can be expressed as $E = Bo \cup To \cup Ss \cup Ca$ where

$$\begin{aligned} Bo &= \{(1, j, k) | 2 \le j \le [W_{max}/2], 1 \le k \le 6\}, \\ To &= \{(1, j, 0) | 2 \le j \le [W_{max}/2]\}, \\ Ss &= \{(i, j, 0) | 2 \le i < j \le [W_{max}/2]\}, \\ Ca &= \{(i, j, 0) | 2 \le j < i \le W_{max}, j \le [W_{max}/2]\}. \end{aligned} \quad (23)$$

B. State-Transition Probabilities

In the Markov chain operation, after every transmission period, there is a state transition. This transition depends on the events occurring in the network. In TCP-Reno, there are two kinds of loss events defined as timeout ($T.O$) and three-duplicate ACKs ($T.D$). We denote the probability of $T.O$ and $T.D$ at congestion window sizes w are $P_{T.O}(w)$ and $P_{T.D}(w)$, respectively. It is noted that a state transition also depends on the phase where the state belongs to.

For the Bo and To phases, because the congestion window is fixed by one, the loss events are always expressed as $T.O$ with congestion window size $w = 1$. In addition, at the last state in Bo phase, when the timeout duration reaches the maximum value (i.e. 2^6T), the state transition definitely

equals one because Bo will be back to To whether or not a loss event occurs.

$$\begin{aligned} P_{(1,j,k)\to(1,j,k+1)} &= P_{T.O}(1), \\ P_{(1,j,k)\to(1,j,0)} &= 1 - P_{T.O}(1), \\ P_{(1,j,6)\to(1,j,0)} &= 1, \\ P_{(1,j,0)\to(1,j,1)} &= P_{T.O}(1), \\ P_{(1,j,0)\to(2,j,0)} &= 1 - P_{T.O}(1). \end{aligned} \tag{24}$$

In the Ss and Co phases, there are three cases that can happen at a state: a loss is detected as $T.O$ ($P_{T.O}$) or $T.D$ ($P_{T.D}$), and no loss ($1 - P_{T.O} - P_{T.D}$). It is also denoted that, when the congestion window size reaches the maximum value, W_{max}, it will stay there if no loss happens. Consequently, the transition matrix in the Ss phase can be expressed as

$$\begin{aligned} P_{(i,j)\to(1,max([i/2],2))} &= P_{T.O}(i), \\ P_{(i,j)\to(max([i/2],2),max([i/2],2))} &= P_{T.D}(i), \\ P_{(i,j)\to(2i,j)} &= 1 - P_{T.D}(i) - P_{T.O}(i). \end{aligned} \tag{25}$$

Similarly, the transition matrix in the Co phase can be given by

$$\begin{aligned} P_{(i,j)\to(1,max([i/2],2))} &= P_{T.O}(i), \\ P_{(i,j)\to(max([i/2],2),max([i/2],2))} &= P_{T.D}(i), \\ P_{(i,j)\to(i+1,j)} &= 1 - P_{T.D}(i) - P_{T.O}(i), \\ P_{(W_{max},[\frac{W_{max}}{2}])\to(W_{max},[\frac{W_{max}}{2}])} &= 1 - P_{T.D}(W_{max}) - \\ &\quad - P_{T.O}(W_{max}). \end{aligned} \tag{26}$$

From Eqs. (24)–(26), the complete transition matrix of the Markov chain cam be obtained if $P_{T.O}(w)$ and $P_{T.D}(w)$ are known. As master of fact, loss-event detection of $T.O$ or $T.D$ is based on the number of losses occurring at a given congestion window size. Based on the study in [18], $P_{T.O}(w)$ and $P_{T.D}(w)$ can be approximately calculated as functions of the probability of i losses out of a congestion window size of w (e.g., $P_w(i)$ in Eq. (6)).

$$\begin{aligned} P_{T.O}^{Re} &= \sum_{i=3}^{w} P_w(i); P_{T.D}^{Re} = P_w(1) + P_w(2), w \geq 10, \\ P_{T.O}^{Re} &= \sum_{i=2}^{w} P_w(i); P_{T.D}^{Re} = P_w(1), 4 \leq w < 10, \\ P_{T.O}^{Re} &= 1 - P_w(0); P_{T.D}^{Re} = 0, w < 4. \end{aligned} \tag{27}$$

Finally, our model is expanded for TCP-SACK and TCP-Tahoe. The detailed operation of these TCP versions can be found in [18]–[20]. The main difference between TCP-SACK and Reno is that selective retransmissions are used by TCP-SACK when multiple segments are lost within a RTT. While in TCP-Tahoe, loss events are observed by timeout for all cases of loss. Our Markov chain therefore can be easily expanded for TCP-SACK and Tahoe by modifying transition probabilities. For example, for TCP-Tahoe we will set $P_{T.D}^{Ta}$ and $P_{T.O}^{Ta}$ by zero and ($P_{T.O}^{Re} + P_{T.D}^{Re}$), respectively. Meanwhile, for TCP-SACK a closed form expression of transition probabilities has been derived in [20] for $w \geq 4$ as follows

$$\begin{aligned} P_{T.O}^{SA} &= \sum_{i=1}^{w-3} P_w(i)(1 - (1 - P_1(1))^i) + \sum_{i=w-2}^{w} P_w(i), \\ P_{T.D}^{SA} &= \sum_{i=1}^{w-3} P_w(i)(1 - P_1(1))^i + \sum_{i=w-2}^{w} P_w(i), \end{aligned} \tag{28}$$

in case of $w < 4$, transition probabilities of TCP-SACK and TCP-Reno are the same.

V. TCP Performance

In the Markov chain model, we denote N as the total number of states (e.g. $N = 27$ in Fig. 2). Let P = [p_1 p_2 ... p_N] be the matrix of steady-state probabilities, where p_i is the probability of the i-th state in the equilibrium. Generally, following Markov chain theory, we have

$$\begin{cases} P = P \times Q \\ \sum_{i=1}^{N} p_i = 1, \end{cases} \tag{29}$$

where $Q = [q_{ij}]_{N\times N}$ is the transition matrix of the Markov chain with an element q_{ij} being the transition probability from the state i to the state j. In our analysis, the transition matrix has been obtained in Section IV.

We can transform Eq. (29) into a basic set of linear equations formed as: $Ax = b$ and then solve it by using standard Gaussian elimination. Here, $x = [p_1\ p_2\ ...\ p_N]^T$, $b = [0\ 0\ ...\ 1]^T$ and $A = [a_{ij}]_{N\times N}$ where a_{ij} is given as

$$\begin{cases} a_{ii} = q_{ii} - 1, \forall\ 1 \leq i \leq N, \\ a_{ij} = q_{ij}, \forall\ 1 \leq i \leq N-1,\ 1 \leq j \leq N \text{ and } i \neq j, \\ a_{Nj} = 1, \forall\ 1 \leq j \leq N. \end{cases} \tag{30}$$

A. TCP Throughput

Let $W = [w_1, w_2, ..., w_N]$ and $T = [t_1, t_2, ..., t_N]$ be the matrices of congestion window sizes and time durations that the TCP spends in N states, respectively. Elements of the first vector are values of the first dimension (i) of Markov chain that we mentioned in Eq. (23). Elements of T can be obtained from the average end-to-end transmission delay (e.g., $E[RTT]$ in Eq. (21)) as follows.

$$\begin{cases} t_n = E[RTT], \forall n \in (To, Ss, Ca), \\ t_n = 2^k T, \forall n \in Bo, 1 \leq k \leq 6, \end{cases} \tag{31}$$

where T is the minimum value of timeout, and generally $T = 5 \times E[RTT]$ is chosen [19]. According to the Little's law, the TCP throughput, which is the ratio between the average congestion window size and the average value of the window holding time, can be given by

$$\Lambda = \frac{W \times x}{T \times x}. \tag{32}$$

B. Joint Throughput-Energy Efficiency

From the previous Section, it is seen that the TCP throughput can be described as a function of the peak transmitted power and the maximum number of re-transmissions: $\Lambda = f(P_s, M)$. Therefore, for a given FSO link, if other parameters are fixed, P_s and M can be set by the transmitter side to increase Λ. Obviously, the higher P_s and M could result in the higher Λ. This, however, also causes extra energy consumption.

In order to analyze combined effect of power management and ARQ-SR on both TCP throughput and energy consumption, we consider a new parameter called joint throughput-energy efficiency, denoted as $J_{\Lambda,E}$. $J_{\Lambda,E}$ is defined as the ratio between the TCP throughput and the average value of the energy consumed for transmitting a data unit of TCP, and can be given as

$$J_{\Lambda,E} = \frac{\Lambda}{E[energy]}. \tag{33}$$

For SC-BPSK modulation, the bit power equals to a half of the peak-transmitted power. Moreover, by applying the previous calculation of the average number of re-transmissions (e.g., Eq. (14)), the average value of the energy consumed for transmitting a TCP segment can be obtained by

$$E[energy] = (\overline{M}+1)L_{TCP}P_s/2 = (\frac{P_f}{1-P_f} - \frac{(M+1)P_f^{M+1}}{1-P_f^{M+1}} + 1)L_{TCP}P_s/2. \quad (34)$$

VI. Numerical Results and Discussions

In this Section, using the previously derived formulations, we analyze the TCP performance over FSO turbulence channels when the ARQ-SR scheme is used at the link layer. Table I shows the system parameters and constants used in the numerical analysis. To focus on the impact of the FSO link on TCP performance, we assume that there is no segment loss in the wired network part ($P_{wire} = 0$). Also, the one-way transmission time in the wired network part, T_{wire}, is fixed by 60 ms.

Regarding the FSO link, we assume the log-normal and gamma-gamma models for the weak-to-moderate and strong turbulence conditions, respectively. In the bit-error probability calculation (i.e., Eqs. (15) and (18)), we assume the receiver noise variance, $\sigma_N^2 = 1.5 \times 10^{-13}$ so that SNR can be obtained by Eq. (11).

TABLE I
System Parameters and Constants

Name	Symbol	Value
TCP segment size	L_{TCP}	536 bytes
Frame size	L_f	268 bytes
Wired part transmission time	T_{wire}	60 ms
CRC checking time	T_{CRC}	10 ms
Transmission rate	R	2 Gb/s
Modulation index	m	1
Responsivity	$\Re$	1
Receiver aperture diameter	D	0.02 m
Atmospheric extinction coefficient	β	0.1 dB/km
Angle of divergence	ϕ	10^{-3} radian

First, in Fig. 3, we compare the performance of TCP-Tahoe, TCP-Reno and TCP-SACK when ARQ-SR is not used. We set the turbulence strength $C_n^2 = 5 \times 10^{-15}$ m$^{-2/3}$ and channel distance $L = 1200$ m for two values of maximum window size ($W_{max} = 16$ and 10 segments). It is seen that when the peak transmitted power increases, the throughput increases until it reaches a limit. This maximum throughput, Λ_{max}, is determined by the value of W_{max}. The systems with higher W_{max} obviously achieve the higher maximum throughput. For instance, Λ_{max} equals 108 kB/s and 68 kB/s when $W_{max} = 16$ and $W_{max} = 10$ segments, respectively.

In addition, we observe that, compared to TCP-Tahoe, both TCP-Reno and TCP-SACK have significantly better performance. This is thanks to the selective re-transmission algorithm used by TCP-SACK and the classification of loss events employed by TCP-Reno, by which a loss can be accurately detected as either $T.O$ or $T.D$ [18]–[20]. In remaining discussions, we employ the TCP-Reno due to its popularity and ability to offer the high performance. The value of

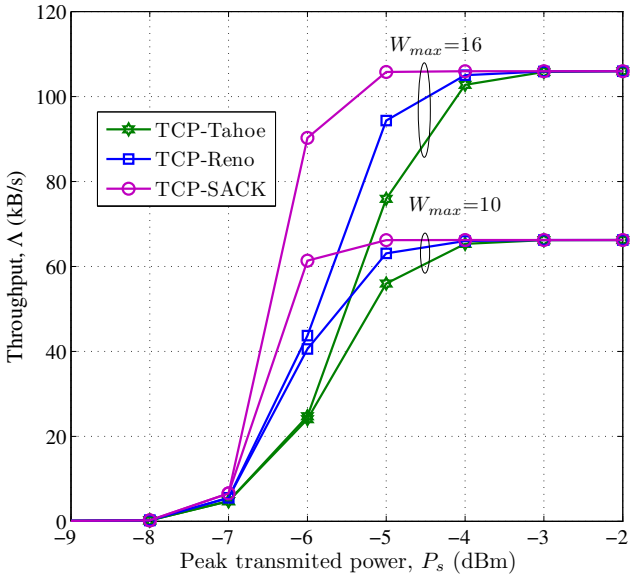

Fig. 3. Throughput versus the peak transmitted power (P_s) for different TCP versions when $C_n^2 = 5 \times 10^{-15}$ m$^{-2/3}$, $L = 1200$ m and no ARQ-SR.

maximum window size $W_{max} = 16$ segments, which is widely used in related studies, is also selected.

Figures 4, 5 and 6 show the system throughput versus the peak transmitted power with different maximum number of re-transmissions and channel distances for weak, moderate and strong turbulence regimes, respectively. The turbulence strength C_n^2 is selected as follows: $C_n^2 = 5 \times 10^{-15}$ m$^{-2/3}$ for the weak turbulence, $C_n^2 = 9 \times 10^{-15}$ m$^{-2/3}$ for the moderate turbulence, and $C_n^2 = 4 \times 10^{-14}$ m$^{-2/3}$ for the strong turbulence. Two channel distances of 1000 m and 1500 m are considered. Using these figures, the impact of ARQ-SR, turbulence strength, channel distances and the peak transmitted power on TCP throughput can be comprehensively analyzed.

As is evident, the increase of turbulence strength results in the increase of the required peak transmitted power to achieve the same throughput. For example, in the case of no ARQ-SR and $L = 1000$ m, in order to obtain the maximum throughput ($\Lambda_{max} = 108$ kB/s), the required P_s are -6 dBm, -2 dBm and 10 dBm for weak, moderate and strong turbulences, respectively. Additionally, the system performance also depends strongly on the channel distance. More specifically, an increase in L by 500 m leads to an increase of the required peak transmitted power by approximately 10 dB to achieve the same Λ_{max}. This phenomenon can be observed in Fig 5.

Next, we highlight the advantage of ARQ-SR scheme to improve the TCP throughput by comparing the performance of the system in various cases of M. It is seen that when ARQ-SR is employed, lower P_s is required to achieve the maximum throughput. For example, in Fig. 6 if ARQ-SR with $M = 2$ is employed, the maximum throughput can be achieved even when $P_s = 0$ dBm whereas the FSO system without ARQ-SR requires $P_s = 10$ dBm to reach that throughput.

More importantly, the increase of M also further improves TCP throughput. As a result, the required P_s to reach the maximum throughput decreases as M increases, especially

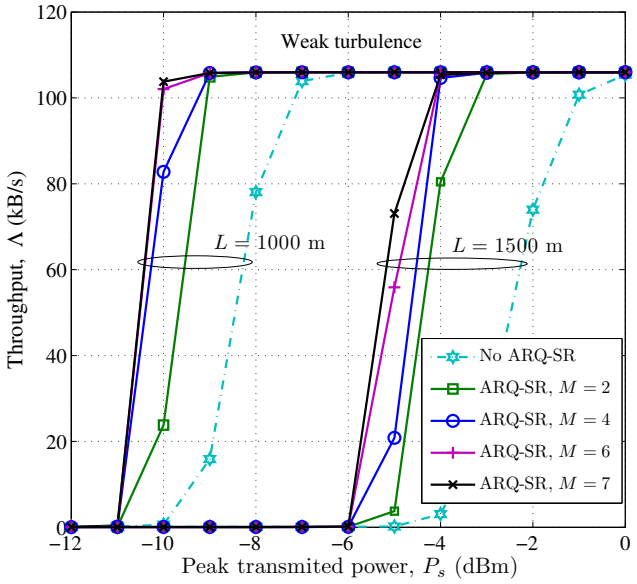

Fig. 4. Throughput versus the peak transmitted power (P_s) for different values of M and L when $C_n^2 = 5 \times 10^{-15}$ m$^{-2/3}$.

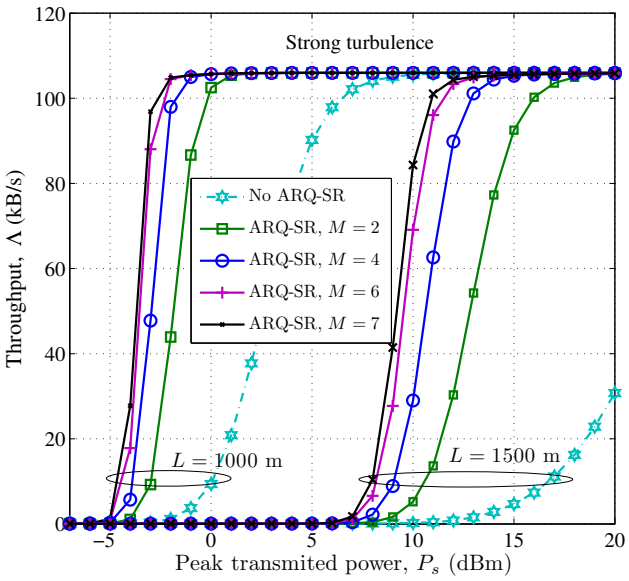

Fig. 6. Throughput versus the peak transmitted power (P_s) for different values of M and L when $C_n^2 = 4 \times 10^{-14}$ m$^{-2/3}$.

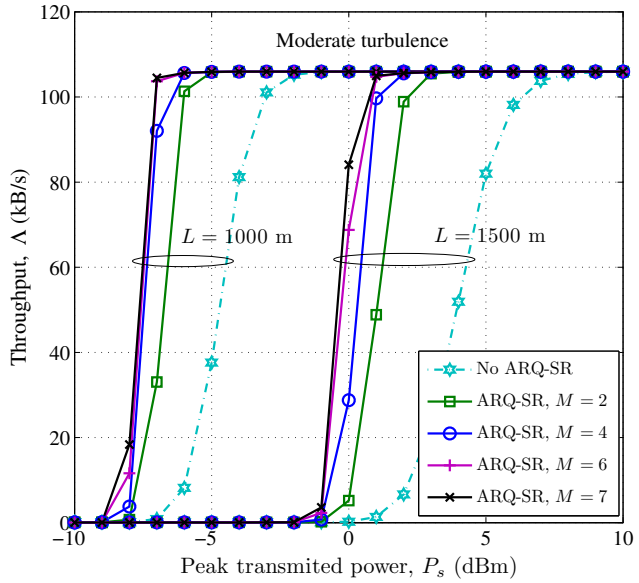

Fig. 5. Throughput versus the peak transmitted power (P_s) for different values of M and L when $C_n^2 = 9 \times 10^{-15}$ m$^{-2/3}$.

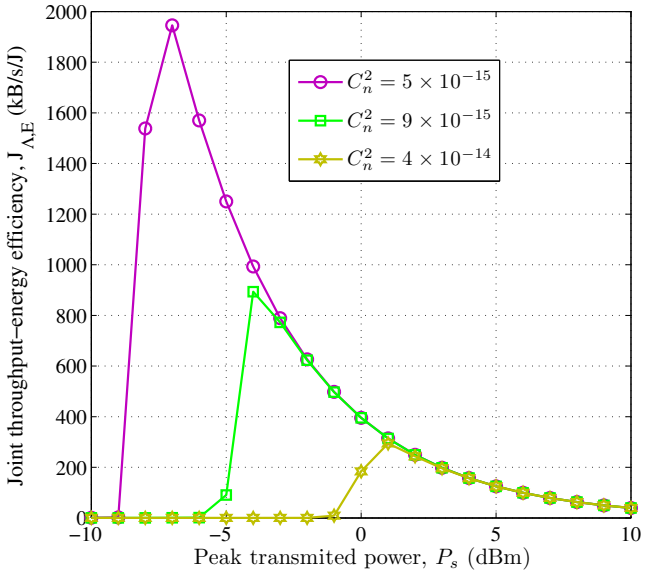

Fig. 7. Joint throughput-energy efficiency versus the peak transmitted power (P_s) for different turbulence strengths when $L = 1200$ m and $M = 6$.

in case of strong turbulence as shown in Fig. 6. However, this required power remains unchanged when M becomes higher than 6. This is because while the use of ARQ-SR decreases the TCP segment-loss probability, it significantly increase the average end-to-end transmission delay caused by the re-transmission. It is therefore recommended that $M = 6$ is the optimized value for analyzed systems.

In Figs. 7 and 8, we analyze the joint throughput-energy efficiency, $J_{\Lambda,E}$ when the optimal value of maximum number of re-transmissions, $M = 6$, is used. The purpose is to find the range of transmitted powers at which the acceptable throughput-energy efficiency is attained under the impact of different turbulence strengths, channel distances and the peak transmitted powers. More specifically, Fig. 7 shows $J_{\Lambda,E}$ vs. the peak transmitted power, P_s, for different turbulence strengths, when $L = 1200$ m; $J_{\Lambda,E}$ vs. P_s for various channel distances with $C_n^2 = 9 \times 10^{-15}$ m$^{-2/3}$ is shown in Fig. 8.

It is intuitively clear in all Figures that there exists an optimal value of peak transmitted power, P_{op}, at which the joint throughput-energy efficiency is maximized. The presence of P_{op} is due to the fact that when the peak transmitted power becomes high enough, the TCP throughput saturates, and the further increase of P_s only results in additional energy consumption.

In Fig. 7, it is seen that as the turbulence strength increases, the optimal peak transmitted power P_{op} increase whereas the joint throughput-energy efficiency $J_{\Lambda,E}$ decease. For instance, when $C_n^2 = 5 \times 10^{-15}$ m$^{-2/3}$, we have $P_{op} = -7$ dBm and the maximum joint throughput-energy efficiency

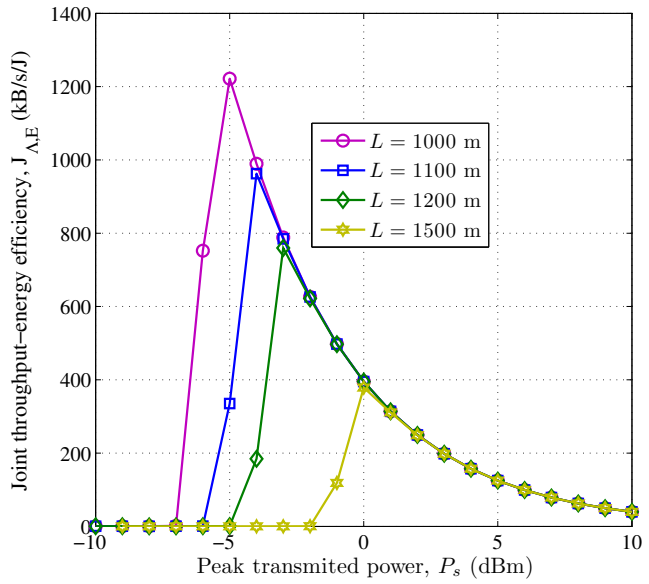

Fig. 8. Joint throughput-energy efficiency versus the peak transmitted power (P_s) for different channel distances when $C_n^2 = 9 \times 10^{-15}$ $\mathrm{m}^{-2/3}$ and $M = 6$.

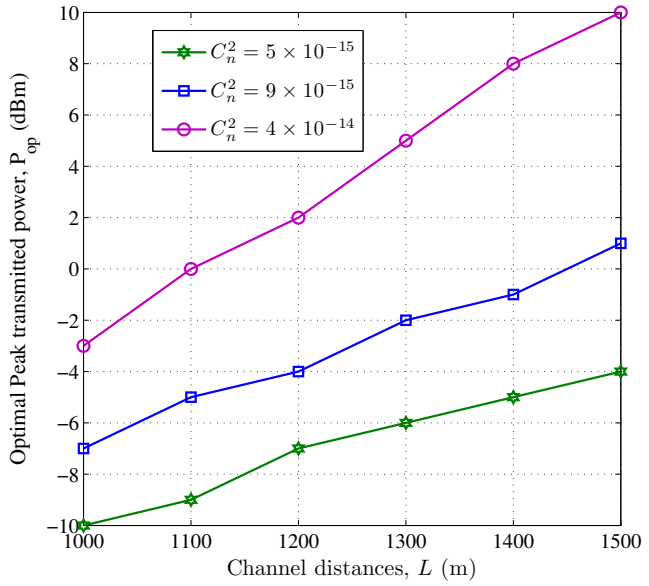

Fig. 9. The optimal peak transmitted power versus the channel distance (L) for different turbulence strengths when $M = 6$.

$J_{\Lambda,E} = 1950$ kB/s/J can be achieved. However, at $C_n^2 = 9 \times 10^{-15}$ $\mathrm{m}^{-2/3}$, the transmitted power of -4 dBm is required to achieve the maximum $J_{\Lambda,E}$ of approximately 900 kB/s/J. The reason is that, as the turbulence strength increases, higher transmitted power is required to reach the SNR value at which the maximum throughput can be achieved. In addition, as the system P_s increases, additional energy is also required for transmitting an unit data of TCP. As a result, the joint throughput-energy efficiency is decreased.

The effect of channel distances on the joint throughput-energy efficiency is analyzed in Fig. 8. Obviously, the optimal peak transmitted power changes frequently when the channel distances varies. When the channel distance increases from 1000 m to 1500 m, it is seen that the optimal peak transmitted power also varies between -5 dBm and 0 dBm. Moreover, if we continue to increase the peak transmitted power (higher than 0 dBm), the joint throughput-energy efficiencies start decreasing, and they are the same for different channel distances. This is because in this case when the transmitted power is high enough, the TCP throughput reaches the maximum for any channel distances and the joint throughput-energy efficiency takes the same value for different distances.

Finally, we combine results of Fig. 7 and Fig. 8 in Fig. 9. Using this figure, we can find the optimal peak transmitted power for a specific turbulence strength and channel distance. Again, it is confirmed that to achieve the maximum joint throughput-energy efficiency, the optimal peak transmitted power should be increased when the channel distance increases. The higher turbulence strength requires the higher value of P_{op}. This figure allows us to select the range of optimal transmitted power for a given the channel distance. For example, when the channel distance is 1300 m, the range of of optical transmitted power is from -6 to 5 dBm.

VII. Conclusions

We have analytically studied the performance of TCP over FSO links with ARQ-SR used in the link layer. A 3-D Markov chain model with the exponential back-off phase was used to derive the TCP throughput and joint throughput-energy efficiency for TCP-Tahoe, Reno and SACK. Various physical and link layers parameters, including turbulence strength, channel distance, transmitted power, and the ARQ-SR maximum number of re-transmissions, were taken into account in the TCP performance analysis. Numerical results showed that the impact of turbulence and channel distance on the TCP throughput are severe. However, using ARQ-SR scheme could significantly reduce the required transmitted power to reach the maximum throughput. It was also shown that the recommended value of the maximum number of re-transmissions is 6 for the link layer of the analyzed system. In addition, the optimal peak transmitted power for the physical layer was investigated by considering the joint throughput-energy efficiency under the impact of atmospheric turbulence and channel distance. The results revealed the relation between the channel distance, the turbulence strength and the optimal peak transmitted power for the joint throughput-energy efficiency.

References

[1] O'Brien, D., and Katz, M., "Optical wireless communications within fourth-generation wireless systems', J. Opt. Netw., 2005, 4, pp. 312–322.
[2] Xiaoming Zhu; Kahn, J.M., "Free-space optical communication through atmospheric turbulence channels," Communications, IEEE Transactions on , vol.50, no.8, pp. 1293–1300, Aug 2002.
[3] Uysal, M., Li, J.T., and Yu, M., "Error rate performance analysis of coded free-space optical links over gamma-gamma atmospheric turbulence channels", IEEE Trans. Wireless Commun., 2006, 5, (6), pp. 1229–1233.
[4] Xuegui Song; Mingbo Niu; Cheng, J., "Error Rate of Subcarrier Intensity Modulations for Wireless Optical Communications," Communications Letters, IEEE , vol.16, no.4, pp.540–543, April 2012.
[5] W. Popoola, Z. Ghassemlooy, H. Haas, E. Leitgeb, and V. Ahmadi, "Error performance of terrestrial free space optical links with subcarrier time diversity," IET Commun. 6, 499 (2012).

[6] Bayaki, E.; Schober, R.; Mallik, R.K., "Performance analysis of MIMO free-space optical systems in gamma-gamma fading," Communications, IEEE Transactions on , vol.57, no.11, pp.3415–3424, Nov. 2009.
[7] Luong, D.A.; Cong Thang Truong; Pham, A.T., "Effect of APD and thermal noises on the performance of SC-BPSK/FSO systems over turbulence channels," Communications (APCC), 2012 18th Asia-Pacific Conference on, pp.344–349, Oct. 2012.
[8] Chunlei Liu; Jain, R., "Approaches of wireless TCP enhancement and a new proposal based on congestion coherence," System Sciences, 2003. Proceedings of the 36th Annual Hawaii International Conference on , pp.10, Jan. 2003.
[9] Wenqing Ding; Jamalipour, A., "A new explicit loss notification with acknowledgment for wireless TCP," Personal, Indoor and Mobile Radio Communications, 2001 12th IEEE International Symposium on , vol.1, no., pp.B-65,B-69 vol.1, Sep. 2001.
[10] Chaskar, H.M.; Lakshman, T. V.; Madhow, U., "TCP over wireless with link level error control: analysis and design methodology," Networking, IEEE/ACM Transactions on , vol.7, no.5, pp.605–615 Oct. 1999.
[11] Le, L.; Hossain, E.; Le-Ngoc, T., "Interaction between radio link level truncated ARQ, and TCP in multi-rate wireless networks: a cross-layer performance analysis," Communications, IET , vol.1, no.5, pp.821–830, Oct. 2007.
[12] Mahmudul Haque, A.H.M.; Mondal, N.I.; Ghosh, S.K.; Bhotto, M.Z.A., "End to End Adaptive Forward Error Correction (FEC) for Improving TCP Performance over Wireless Link," Electrical and Computer Engineering, 2006. ICECE '06. International Conference on , vol., no., pp.569–572, Dec. 2006.
[13] Lee, E.J.; Chan, V.W.S., "Performance of the transport layer protocol for diversity communication over the clear turbulent atmospheric optical channel," Communications, 2005. ICC 2005.
[14] Kose, C.; Halford, T.R., "Incremental redundancy hybrid ARQ protocol design for FSO links," Military Communications Conference, 2009. MILCOM 2009. IEEE, pp.1–7, Oct. 2009.
[15] Kiasaleh, K., "Hybrid ARQ for FSO Communications Through Turbulent Atmosphere," Communications Letters, IEEE, vol.14, no.9, pp.866–868, Sep. 2010.
[16] Hammons, A.R.; Davidson, F., "On the design of automatic repeat request protocols for turbulent free-space optical links," Military Communications Conference, 2010 - MILCOM 2010, pp.808–813, Oct. 31–Nov. 3 2010.
[17] Kumar, A., "Comparative performance analysis of versions of TCP in a local network with a lossy link," Networking, IEEE/ACM Transactions on , vol.6, no.4, pp.485-498, Aug 1998.
[18] Sikdar, B.; Kalyanaraman, S.; Vastola, K.S., "Analytic models for the latency and steady-state throughput of TCP Tahoe, Reno, and SACK," Networking, IEEE/ACM Transactions on , vol.11, no.6, pp. 959- 971, Dec. 2003.
[19] Casetti, C.; Meo, M., "A new approach to model the stationary behavior of TCP connections," INFOCOM 2000. Nineteenth Annual Joint Conference of the IEEE Computer and Communications Societies. Proceedings. IEEE , vol.1, pp.367-375 vol.1, 2000.
[20] Wierman, A.; Osogami, T., "A unified framework for modeling TCP-Vegas, TCP-SACK, and TCP-Reno," Modeling, Analysis and Simulation of Computer Telecommunications Systems, 2003. MASCOTS 2003. 11th IEEE/ACM International Symposium on , pp. 269- 278, 12-15 Oct. 2003.